LUND UNIVERSITY

Study of the Average Charge States of 188Pb and 252,254No Ions at the Gas-filled Separator TASCA

Khuyagbaatar, J.; Ackermann, D.; Andersson, Lise-Lotte; Ballof, J.; Bruechle, W.; Duellmann, Ch. E.; Dvorak, J.; Eberhardt, K.; Even, J.; Gorshkov, A.; Graeger, R.; Hessberger, F. -P.; Hild, D.; Hoischen, Robert; Jaeger, E.; Kindler, B.; Kratz, J. V.; Lahiri, S.; Lommel, B.; Maiti, M.; Merchan, E.; Rudolph, Dirk; Schaedel, M.; Schaffner, H.; Schausten, B.; Schimpf, E.; Semchenkov, A.; Serov, A.; Tuerler, A.; Yakushev, A.

Link to publication

Study of the average charge states of ^{188}Pb and ^{252,254}No ions at the gas-filled separator TASCA

J. Khuyagbaatar^{a,b}, D. Ackermann^a, L.-L. Andersson^{c,1}, J. Ballof^d, W. Brüchle^a, Ch. E. Düllmann^{a,b,d}, J. Dvorak^{a,b}, K. Eberhardt^d, J. Even^d, A. Gorshkov^e, R. Graeger^e, F.-P. Heßberger^{a,b}, D. Hild^d, R. Hoischen^{a,c}, E. Jäger^a, B. Kindler^a, J.V. Kratz^d, S. Lahiri^f, B. Lommel^a, M. Maiti^f, E. Merchan^{a,c,g}, D. Rudolph^c, M. Schädel^a, H. Schaffner^a, B. Schausten^a, E. Schimpf^a, A. Semchenkov^{a,2}, A. Serov^h, A. Türler^{e,3}, A. Yakushev^{e,4}

^{a}GSI Helmholtzzentrum für Schwerionenforschung GmbH, 64291 Darmstadt, Germany
^{b}Helmholtz Institut Mainz, 55099 Mainz, Germany
^{c}Lund University, 22100 Lund, Sweden
^{d}Johannes Gutenberg-Universität Mainz, 55099 Mainz, Germany
^{e}Technische Universität München, 85748 Garching, German
^{f}Saha Institute of Nuclear Physics, Kolkata-700064, India
^{g}Universidad Nacional de Colombia, Bogotá, Colombia
^{h}Paul Scherrer Intitute, 5232 Villigen, Switzerland

Abstract

The average charge states of ^{188}Pb and ^{252,254}No ions in the dilute helium gas were measured at the gas-filled separator TASCA. Hydrogen gas was also used as a filling gas for measurements of the average charge states of ^{254}No. Helium and hydrogen gases at pressures from 0.2 mbar to 2.0 mbar were used. A strong dependence of the average charge states on the pressure of the filling gases was observed for both, helium and hydrogen. The influence of this dependence, classically attributed to the so-called "density effect", on the performance of TASCA was investigated. The average charge states of ^{252,254}No ions were also measured in mixtures of helium and hydrogen gases at low gas pressures around 1.0 mbar. From the experimental results simple expressions for the prediction of the average charge states of heavy ions moving in rarefied helium gas, hydrogen gas, and in their mixture are derived.

Key words: Gas-filled separator, Average charges, Heavy ion, TASCA

1. Introduction

The knowledge on the charge state distribution of heavy ions moving in gas-filled regions is an important issue of heavy-ion beam related physics. This distribution depends on charge-exchange collisions between the heavy ions and atoms of the gas. Already decades ago, many experimental and theoretical investigations have been performed on charge-exchange collisions for light and medium heavy ions in rarefied gases [1]. As results of these works many basic aspects of charge-exchange collisions have been established. Recently, a renewed interest in the understanding of average charge states of heavy ions in rarefied gases has been motivated by the production of heavy and superheavy elements at gas-filled separators [2, 3, 4, 5, 6, 7, 8].

The separation of different ions in gas-filled separators is based on their different magnetic rigidities $B\rho = mv/qe$. B denotes the magnetic flux density, ρ the radius of curvature of the ion trajectory, m and v the mass and velocity of the ion, respectively, q its average (ionic) charge state and e is the elementary charge. The well prediction of the average charge states of the different heavy ions in the filling gas of the separator allows to define the further trajectories of them through the separator.

Several experimental studies of the average charge states of heavy ions have been performed at gas-filled separators to lay the basis for the correct prediction of average charge states of heavy and superheavy ions produced in fusion-evaporation reactions [9, 10, 11, 12, 13, 14]. Semi-empirical expressions were derived, based on a parameterization of the experimental data according to the theoretical underpinnings of charge-exchange collisions, such as an influence of the atomic shell structure of the heavy ions [9, 10, 11, 12, 13, 14]. These investigations were often performed at different pressures of the different facilities, which were, however fixed at a value which was evaluated to be optimum for the respective facility. The influence of a variation of the gas pressure has not been included in any of the above mentioned expressions.

A dependence of the average charge states on the gas pressure has been observed at the Dubna gas-filled recoil separator (DGFRS) [12]. As a possible explanation, a so called "density effect" was invoked, as it is well known from charge-exchange collisions [1]. However, an influence of this effect on the performance of gas-filled separators has not been investigated so far.

At present, gas-filled separators are typically filled with ei-

---

ther pure helium (He) or pure hydrogen (H_2). Hydrogen seems to provide better suppression of background originating from target-like ions [12, 15]. However, as the average charge states in pure H_2 are lower than in pure He, H_2-filled separators necessitate a stronger dipole magnet to bend the more rigid evaporation residues (ERs). The use of a mixture of these two gases allows combining the advantages of both gases, i.e., to retain a good background suppression while keeping rather high average charge states of ERs. However, no data fig1nor formalism to predict the average charge states of heavy ions in gas mixtures exists.

Our present experimental work aimed at studying the average charge states of heavy ions, more specifically ^{188}Pb and ^{252,254}No, in various rarefied gases and their mixtures at the gas-filled TransActinide Separator and Chemistry Apparatus (TASCA) [7, 16, 17, 18, 19] to investigate the influence of the "density effect" on ions of different atomic number, mass and velocity. The measured data provide a basis for the prediction of average charge states in gas mixtures.

2. General aspects of charge-exchange collisions

The charge state distribution of heavy ions passing through a rarefied gas can be described in terms of the fractions of the heavy ions $F_i(x)$ in charge state i, where x refers to the number of gas atoms or molecules per square centimeter traversed by the heavy ion ($\sum_i F_i(x) = 1$). The variation of the charge state fractions is described by a system of differential equations

$$\frac{dF_i(x)}{dx} = \sum_{j, j \neq i} \left[\sigma_{ij} \cdot F_j(x) - \sigma_{ji} \cdot F_i(x) \right] \qquad (1)$$

where, σ_{ij} and σ_{ji} are the cross-sections for electron capture and loss processes [1]. At large values of x the variation of the fractions decreases and may vanish completely, $\frac{dF_i(x)}{dx} \to 0$. This means that the electron capture and electron loss processes between the heavy ions and gas atoms compensate each other and the fraction of each i-th charge state (hereafter: F_i) in the heavy ions will not change anymore. This situation gives the distributions of equilibrated charge states (average charge state) of heavy ions. From this point of view the average charge state is determined as:

$$\bar{q} = \sum_i q_i \cdot F_i \qquad (2)$$

In principle, equations (1) and (2) allow to calculate the average charge states of heavy ions as well as average charge state distribution. However, the knowledge on the electron capture and loss cross-sections of heavy ions in rarefied gases is still scarce. First attempts to theoretically describe the average charge state of heavy ions moving in a rarefied gas were performed in 1940 by Bohr [20] and Lamb [21] in studies of fission fragments.

Bohr assumed that a heavy atom moving rapidly through a rarefied gas retains all of its electrons that have orbital velocities exceeding that of the velocity of the atom relative to the medium. Applying the Thomas-Fermi model for the structure of the atom, he then obtained the well-known dependence of the average charge state $\bar{q}$ of a heavy ion with atomic number Z on its velocity v,

$$\bar{q} = (v/v_0) \cdot Z^{1/3} \qquad (3)$$

for a velocity range $1 < (v/v_0) < Z^{2/3}$. Here, $v_0 = 2.193 \cdot 10^6$ m/s is the velocity of the electron in Bohr's model of the hydrogen atom.

In the work of Lamb the average charge states of fission fragments have been calculated using energy considerations. He assumed that a fragment moving through a rarefied gas with a velocity v "will be stripped down until the ionization potential of the next stage of ionization is greater than the kinetic energy of electrons bombarding the fragment with a velocity v" [21].

In principle, these relatively simple concepts of the average charge state are valid when the time between two subsequent collisions between the heavy ion and a gas atom or molecule is long enough that all excited electrons de-excite to the ground state. However, this is true only at low gas pressures with the number of collisions between the heavy ions and gas atoms or molecules being rare. The probability of collisions between excited heavy ions and species of the filling gas is not negligible in a wide range of gas pressures. This becomes more significant as the time between subsequent collisions becomes comparable to the lifetime of the excited states in the atomic shell. Heavy ions in excited atomic states are bound to more easily lose an electron in a collision with the medium, which leads to an increase of the average charge state with increasing gas pressure. Thus, the real average charge states of heavy ions ($\bar{q}_r$) in the gas will be different from the equilibrated ones ($\bar{q}$) and it can be determined as the sum of $\bar{q}$ and a correction term of the so-called "density effect" ($\bar{q}_r = \bar{q} + \Delta q$).

The "density effect" has been well studied both experimentally and theoretically in the region of light and medium heavy ions (see [1] and reference therein). The maximum "density effect" was estimated by Bohr and Lindhard [22] and their results ($\Delta q = \bar{q}/5$) showed that the real measured average charge states can deviate from the equilibrated ones by up to 20%.

In our simple representation of the correction term for the "density effect" we use an exponential function

$$\Delta q = C_0 \cdot \bar{q} \cdot e^{-\frac{\Delta t}{C_1}} \qquad (4)$$

as an analogy to the radioactive decay law because this effect is related to the de-excitation of the electrons from excited states. C_0 is a constant which can in principle be directly determined to 0.2 according to the Bohr and Lindhard estimates. However, we keep this as a free parameter , which will be fixed by a fit procedure. C_1 is the average lifetime of excited states in the heavy ions, which we assume as a constant value and Δt is the time between two subsequent collisions where electrons of the heavy ions are excited. This time can be written as $\Delta t = kT/(\sqrt{2}\pi d^2 v P)$, where k is the Boltzmann constant, T is the temperature, P is the pressure, d is the diameter of the atoms/molecules, and v is the velocity of the ion. We used

the unit of mbar for the gas pressure P and the dimensionless value of (v/v_0) for the velocity, as it is often practically used at gas-filled separators. A value of $3 \cdot 10^{-10}$ m was taken for the diameter of the heavy atoms and temperature was taken as $30°$. Applying the above mentioned constants and unit conversions the real average charge states of heavy ions including the "density effect" will be:

$$\bar{q}_r = \bar{q}(1 + C_0 \cdot e^{-10^{-11} \cdot \frac{4.61}{C_1 \cdot (v/v_0) \cdot P}}) \tag{5}$$

Here C_0 and C_1 are the above mentioned constants which will be fixed in a procedure. This expression provides the influence of the "density effect" relative to the equilibrated average charge state.

3. Experimental setup

The experiments were performed at the gas-filled recoil separator TASCA [16, 17, 18]. A ^{48}Ca beam was delivered from a 14 GHz ECR ion source and accelerated by the linear accelerator UNILAC to energies of 234.0 and 232.3 MeV. To make use of the highest presently available beam intensities at the UNILAC, TASCA features a windowless differential pumping system [16] and hence, no vacuum window was used. One lead (Z=82) isotope, ^{188}P, and two nobelium (Z=102) isotopes, ^{252,254}No, were produced in the ^{48}Ca+^{144}Sm and ^{48}Ca+^{206,208}Pb fusion-evaporation reactions, respectively. Lead targets were produced in the lead sulfide (PbS) chemical form because of the higher melting point of this compound compared to metallic lead [23]. The isotopic enrichment of ^{206}Pb and ^{208}Pb was 99%. The target material was evaporated onto $\approx 2\,\mu$m thick titanium backing foils. Target thicknesses were $\approx$550 and $\approx$380 μg/cm^2 for the lead and samarium, respectively. All targets were covered with a 10 μg/cm^2 thick carbon layer in order to reduce material losses by sputtering. Three banana-shaped targets were mounted on the rotating target wheel system ARTESIA (A Rotating Target wheel for Experiments with Superheavy-element Isotopes at GSI using Actinides as target material). This target wheel rotates at a frequency of 2000 rpm synchronized with the pulsed UNILAC beam (5 ms pulse length, 50 Hz repetition rate). Details about the target arrangement, its operation and the target production can be found in [24, 25]. The isotope ^{188}Pb was produced at the beam energy of $\approx$219 MeV in the center-of-target which corresponds to the four neutron evaporation channel from the compound nucleus ^{192}Pb. The chosen beam energies resulted in center-of-target energies of $\approx$218 MeV and $\approx$216 MeV [26] close to the maxima of the excitation functions of the two neutron evaporation channels from the compound nuclei ^{254,256}No* [27].

The magnetic system of TASCA consists of a dipole and a quadrupole doublet. Evaporation residues were separated from the primary beam and unwanted nuclear reaction products based on their differing magnetic rigidities, $(B\rho)_0$, in the gas-filled dipole [12]. Quadrupole doublet of the TASCA was operated in its ion-optical focusing mode so-called "High Transmission Mode" (HTM) [18]. To control the gas atmosphere in TASCA, commercially available MKS$^{®}$ gas-flow controllers

operated with a LabVIEW$^{®}$ program were used and permitted excellent control and a very high long-term stability of gas flow rates and, more importantly, of the gas pressure in the separator. This was achieved not only for an individual gas like He or H$_2$ but also for gas mixtures. Gases were always flowing from the rear end of the separator towards the target region.

The separated and focused ERs were implanted into an (80×35) mm^2 large 16-strip position-sensitive silicon detector placed at the focal plane of TASCA (focal plane detector). The detector was cooled to temperatures ranging from -10°C to -30°C. Its energy resolution (FWHM) was 50 keV for full energy α particles with an energy of 5.9 MeV, and the detection efficiency for α particles from implanted ERs was 55%. The detector and data acquisition system of TASCA as used in our experiments reported here was similar to the one at the velocity filter SHIP (Separator for Heavy Ion Products) of the GSI, Germany [28].

The real average charge states (hereafter average charge state) were deduced from the measured distributions of ERs in the focal plane detector. The ERs were identified through their characteristic α decays [29]. The ER distribution in the focal plane is Gaussian-like in both, the horizontal and in the vertical direction. The actual magnetic rigidity can be determined from the position of the center of the horizontal distribution. If this is off-center on the detector indicating that the magnetic rigidity is different from the value preset at the separator and the real magnetic rigidity (hereafter magnetic rigidity) of the detected ERs can be estimated using the following expression

$$(B\rho)_r = (B\rho)_0 \cdot \left(1 + \frac{X}{100 \cdot D}\right) \tag{6}$$

where $(B\rho)_0$ is the value of magnetic rigidity of the separator set for the given experiment, and D is the dispersion at the focal plane of TASCA in unit of [mm] per one percent change in $(B\rho)_0$. In the HTM of TASCA the dispersion D is 0.9 mm [18]. The X is the shift of the center of ions distribution relative to the middle of the focal plane detector and it was determined by fitting the experimental data by Gaussian curve (see Fig. 1). The average charge states of the ERs can be found from the following expression [12] using the $(B\rho)_r$ value.

$$(B\rho)_r = 0.0227 \cdot \frac{A \cdot (v/v_0)}{\bar{q}_r} \tag{7}$$

where A is the atomic mass number of the ERs.

4. Results and discussions

4.1. Dependence of average charge states on the gas pressure

As an example, we show in Fig. 1 horizontal distributions of ^{252}No measured at different He pressures. For all measurements, the same magnetic settings centering ions with a magnetic rigidity of $(B\rho)_0$=2.07 Tm in the focal plane were used. At these settings, the ^{252}No ERs are centered in the focal plane at a He pressure of P=0.8 mbar. The experimental data clearly indicate that the position of the center of the distribution is a function of the gas pressure. At pressures lower than 0.8 mbar

the distributions of ERs are shifting to higher magnetic rigidity, indicating that their charge states become lower. At higher pressures, the situation is opposite. Ion optical simulations of the ion trajectories in TASCA were performed using the **T**ASCA Monte-Carlo **SIM**ulation (TSIM) code [30]. In the TSIM code, the average charge states of heavy ions were estimated by using the semi-empirical expression from [13]. This semi-empirical expression was parameterized using the experimental data on average charge states of heavy ions obtained at a He pressure of 0.66 mbar, as it was determined to be optimal for experiments at the Berkeley Gas-filled Separator (BGS) [13]. The results are shown in Fig. 1 as dashed lines. The calculation reproduces well the distribution of ERs at a gas pressure of 0.5 mbar, which is within the systematic uncertainty of $(B\rho)_0$ between BGS and TASCA. However, the calculated distributions do not reflect the shift of the centers of the distributions. It should be noted that a shift of the distribution by the extent shown in Fig. 1 strongly influences the transmission of the ERs through the separator.

The magnetic rigidity can be deduced from these distributions using the expression 6. The results for ^{188}Pb, ^{252}No and ^{254}No ions in He gas are shown in Fig. 2. The magnetic rigidities of ^{254}No ions measured in H_2 are also shown in Fig. 2. Error bars include uncertainties from the determination of the center of the distribution (single strip width=5 mm) and from the dispersion (15%). The magnetic rigidities are nonlinearly increasing with decreasing gas pressure. Moreover, similar behaviour of the magnetic rigidities depend on the gas pressure are visible in Fig. 2.

The average charge states of ^{252}No and ^{254}No ions in He gas as a function of the velocity are shown in Fig. 3. In a first step, the velocity of the ions inside the target was estimated from fusion-evaporation kinematics. Using the SRIM code [26], the velocity at the exit of the target was estimated, and finally, the velocity at the center of the dipole magnet, after having travelled through 603 mm of gas was estimated using the stopping-power tables of [31]. Error bars show the sum of uncertainties from the deduced magnetic rigidities, the magnetic flux density $(B\rho)_0$ (0.8%), and the velocity v ($\approx$2%). The total uncertainty of the velocities was deduced from the uncertainties of the beam energy (0.2%) and the thicknesses of the Ti backing foil (10%) and PbS target (10%), respectively. The variation of velocities in Fig. 3 is due to different beam energies and target thicknesses. The average charge states measured at constant gas pressure (0.8 mbar) show a linear dependence on the velocity, as predicted by expression 3. However, the average charge states at higher and lower gas pressures deviate significantly from the results measured at 0.8 mbar.

From the results presented above the existence of an effect which is related solely to the gas pressure follows. Such a behaviour of the average charge states has been observed earlier at the DGFRS [12] and was explained by the so-called "density effect" [1], as mentioned in [12]. The average charge states can be described using expression 5 as a function of $1/[(v/v_0)P]$. The average charge states are shown in Fig. 4 as a function of $1/[(v/v_0)P]$. However, in our representation of the "density effect" we used the magnetic rigidities which has a smaller relative uncertainties compared to the real average charge states
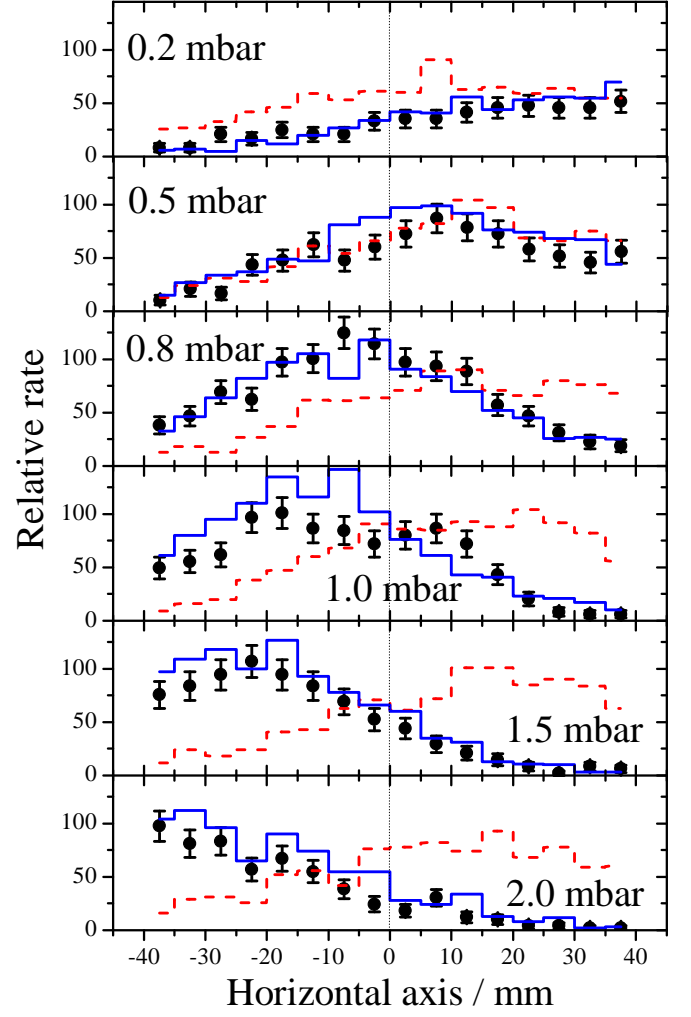

Figure 1: Experimental distributions of ^{252}No at the focal plane detector depending on the He gas pressure. The same magnetic rigidity of $(B\rho)_0$=2.07 Tm was used for TASCA in HTM. Only statistical error bars are shown. Lines are the calculated distributions by the TSIM code [30] using the average charge state predictions from [13] (dashed) and including the "density effect" (solid). See text for details.

(see Fig. 2 and Fig. 4). Similar to $\bar{q}_r$ the reverse magnetic rigidity can be written as a function of $1/[(v/v_0)P]$ combining expressions 5 and 7:

$$\frac{1}{(B\rho)_r} = \frac{1}{0.0227 \cdot A \cdot (v/v_0)} \cdot \bar{q}(1 + C_0 \cdot e^{-10^{-11} \cdot \frac{4.61}{C_1 \cdot (v/v_0) \cdot P}}) \text{ (8)}$$

where A, (v/v_0), and $\bar{q}$ are atomic mass number, velocity, and equilibrated average charge state of heavy ions, respectively. The reverse magnetic rigidities of measured heavy ions are shown in Fig. 5a as a function of $1/[(v/v_0)P]$. The results of fits for each ion are also shown in Fig. 5a by dashed lines.

Results of the fitted curve for ^{188}Pb, which will be used later to provide a general expression for the correction of the "density effect" in the existing semi-empirical expression is given below:

$$\frac{1}{(B\rho)_r} = 0.593 + 0.0652 \cdot e^{-\frac{4.61}{1.8 \cdot (v/v_0) \cdot P}} \tag{9}$$
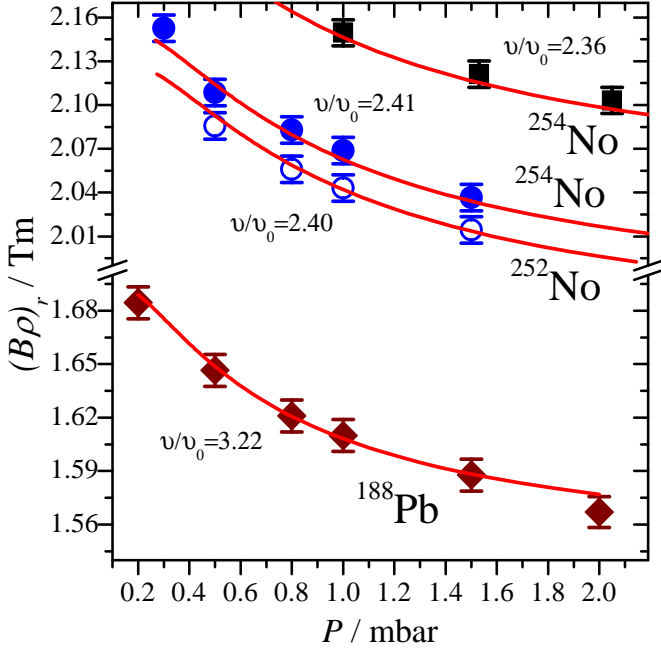
4

Figure 2: Dependence of magnetic rigidities of lead and nobelium evaporation residues on the gas pressure. Full and open circles denote the magnetic rigidities of ^{252}No and ^{254}No in He gas, respectively. Full rectangles denote the magnetic rigidities of ^{254}No in H$_2$ gas. The curves are representing the results of an estimation. See text for details.
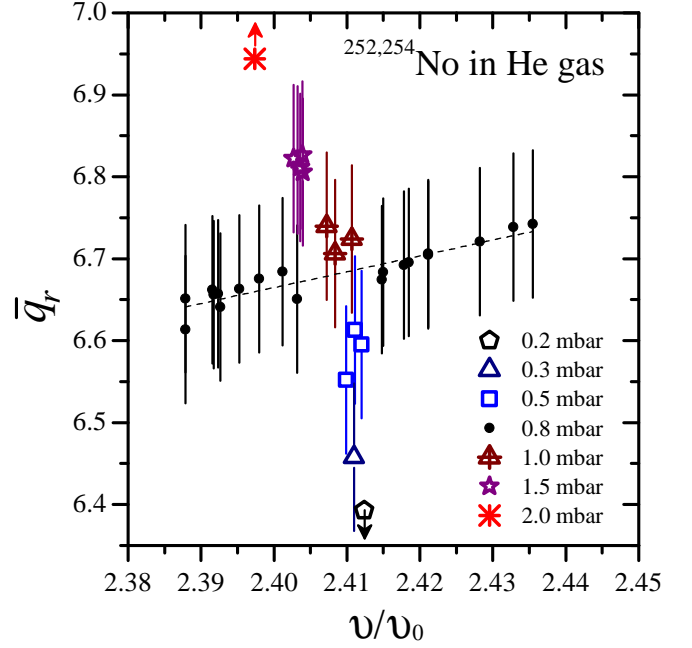

Figure 3: Measured average charge states of ^{252,254}No ions depend on their velocity (expressed in units of the Bohr velocity). The dashed line shows a linear fit of experimental data measured at a gas pressure of 0.8 mbar. Arrows show the lower (up) and higher (down) limits for average charge state values. See text for details.

The shapes of the fitting curves are very similar which indicates that the "density effect" is influencing relatively to the equilibrated average charge states of heavy ions, which are determined from the type of the colliding heavy ion and gas. Based on this feature we made an attempt to parameterize the "density effect" for various heavy ions, various gases, and various velocities. As we mentioned in section 1 typical semi-empirical expressions for the prediction of the average charge states are filled to data taken at a single gas pressure, which is different for the different expressions. Therefore, it is reasonable to find a correction term to the already existing semi-empirical expressions, which takes into account the pressure dependency i.e., the "density effect".

The magnetic rigidities of all measured ions at $(1/[(v/v_0)P])^{fix}$=0.42, which corresponds to Δt=20 ps, were used for the normalization of the measured data.

Normalized reverse magnetic rigidities are shown in Fig. 5b as a function of $1/[(v/v_0)P]$. These values are well lying on one single exponential curve. The data were fitted by the following normalized function:

$$\frac{(B\rho)_r^{fix}}{(B\rho_r)} = C_2 \cdot (1 + C_0 \cdot e^{-10^{-11} \cdot \frac{4.61}{C_1 \cdot (v/v_0) \cdot P}}) \tag{10}$$

where $(B\rho)_r^{fix}$ is the magnetic rigidity estimated by fit functions for each ion (as an example: expression 9 for ^{188}Pb) at the given $(1/[(v/v_0)P])^{fix}$. C_i (i=0,2) are the constants. The results of the fit and its parameters are shown in Fig. 5b. The magnetic rigidities estimated with this function are shown by the solid lines in Fig. 2. The corresponding average charge states can be

found using the following expression.

$$\bar{q}_r = \bar{q}_r^{fix} \cdot (C_2 \cdot (1 + C_0 \cdot e^{-10^{-11} \cdot \frac{4.61}{C_1 \cdot (v/v_0) \cdot P}})) \tag{11}$$

where $\bar{q}_r^{fix}$ is the average charge state at the chosen $(1/[(v/v_0)P])^{fix}$ value (see above).

The results of estimated average charge states of these ions are shown in Fig. 4. The influence of the "density effect" is well describing for all cases.

The expression 11 can be used for other separators which use different parameterized expressions for the prediction of the average charge states at different gas pressures. The estimation of the "density effect" at other separators can be done by correcting expression 11. Let's assume that there is a semi-empirical expression at a gas filled separator and it gives the $\bar{q}_{s.emp}$ at the optimal gas pressure P_{sep} of separator. In this case the average charge state can be found as:

$$\bar{q}_r = \bar{q}_{s.emp} \cdot \frac{0.614}{(B\rho)_{sep}} \cdot (0.96 + 0.1 \cdot e^{-\frac{2.09}{(v/v_0) \cdot P}}) \tag{12}$$

where 0.614 and is the value of the reverse magnetic rigidity at $(1/[(v/v_0)P])^{fix}$=0.42 for ^{188}Pb estimated by expression 9. $(B\rho)_{sep}$ is the estimated reverse magnetic rigidity at the given gas pressure P_{sep} and velocity (v/v_0) of heavy ions by expression 9 at the particular separator. This simple expression can be used to estimate the influence of the "density effect" at various gas-filled separators.

The obtained parameterized expressions are useful for the estimation of average charge states of heavy ions passing through
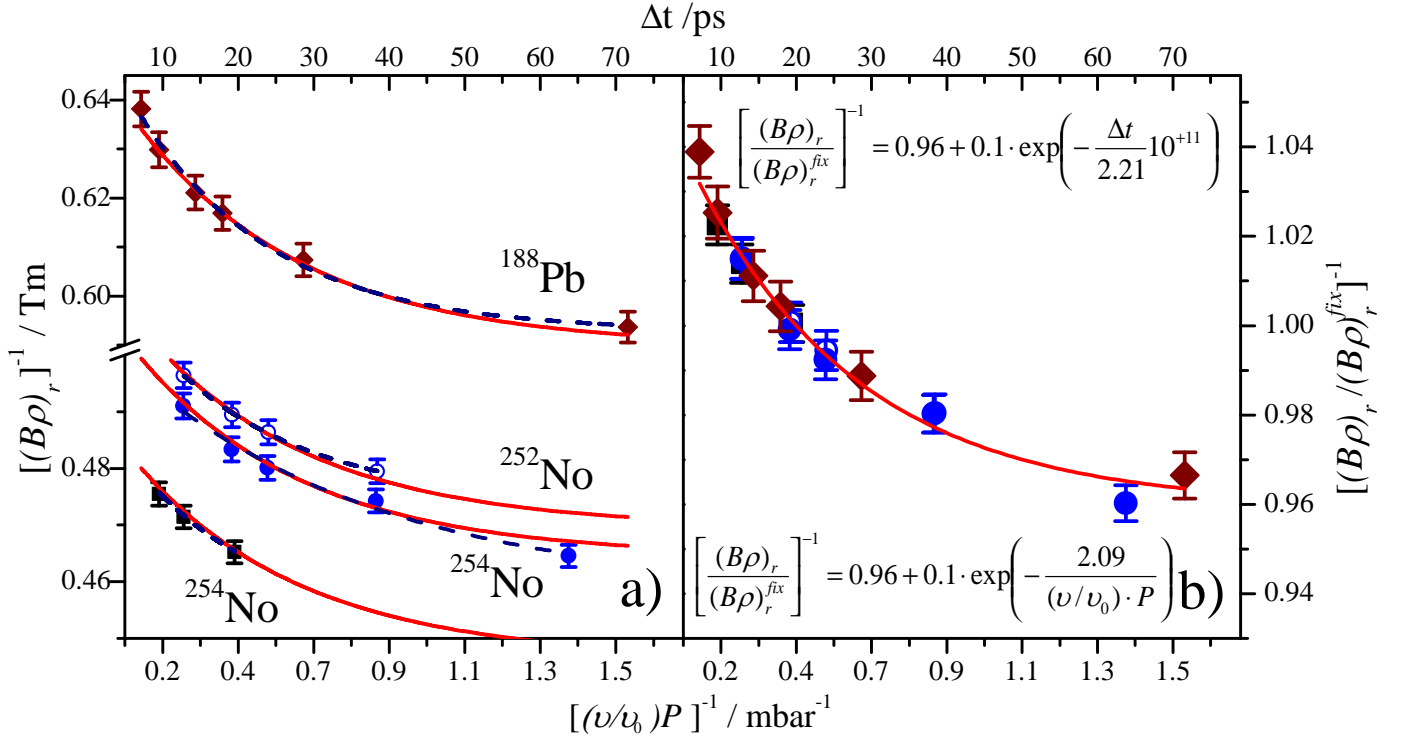
5

Figure 5: Dependence of reserve magnetic rigidities a) and b) normalized reverse magnetic rigidities of lead and nobelium evaporation residues on $1/[(\upsilon/\upsilon_0)P]$ (bottom horizontal axis) i.e., time between the consequence collisions Δt (top horizontal axis). The dashed curves represent the results of a fit of data plotted in a). The solid curves represent the results of a fit of data plotted in b). Normalized fit functions with fitted parameters are given in b). See text for details.
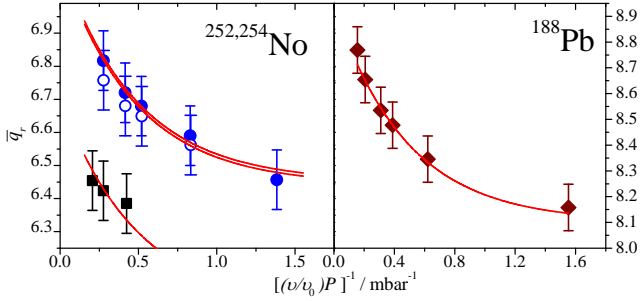

Figure 4: The average charge states of ^{252}No and ^{254}No ions depend on $1/[(\upsilon/\upsilon_0)P]$. left) Full and open circles denote average charge states of ^{254}No and ^{252}No in He gas, respectively. Full rectangles denote the average charge states of ^{254}No in H_2 gas. right) Full symbols denote the average charge states of ^{188}Pb in He gas. The curves represent the results of an estimation. See text for details.

TASCA. Results of TSIM calculations are shown in Fig. 1. The average charge states of heavy ions in the TSIM calculation were estimated using the parametrization from [13], which neglects the "density effect" (dashed lines) and with expression 12, which includes the "density effect" (solid line) relative to the estimated average charge states from [13]. The calculations based on expression 12 describe the experimental distributions of ERs over a wide pressure range well. The results also well describe the width of the ER distributions. As mentioned before, the "density effect" originates from excitations of electrons in the atomic shells and, therefore, it has no influence on the collision kinematics (angular spread) between the heavy ions and atoms of the gas.

4.2. The average charge states of heavy ions in gas mixtures

The average charge states of ^{254}No ions were measured in mixtures of He and H_2. The ratio of the numbers of He to H_2 atoms ($\nu = n_{He}/n_{H_2}$) were established by controlling the gas flow rate of each gas. The total pressure of these mixtures was measured. The average charge states i.e., the magnetic rigidities, were measured at gas mixture ratios of $\nu=1, 2, 3,$ and 4 at various pressures. The results are shown in Figs. 6 and 7 as a function of $1/[(\upsilon/\upsilon_0)P]$.

First of all, the "density effect" is also observed in gas mixtures. The estimated average charge states/magnetic rigidities of ^{254}No ions in pure He and pure H_2 are included in Fig. 6 and Fig. 7 for reference (dashed lines). The average charge states/magnetic rigidities of ^{254}No ions traveling through gas mixtures lie in between these curves, and their absolute values depends on the ratio of the two gases.

Let us now consider the formalism of charge-exchange collisions in terms of charge state fractions $F_i(x)$ (see Sect. 2). In the case of pure He (H_2) gas, the equilibrated charge states are reached at large values of x, and their distribution is determined by fractions $F_i^{He}(x)$ and $F_i^{H_2}(x)$). In the case of different types of gas atoms, each fraction of the i-th charge state of heavy ions will have a probability $p(He) = n_{He}/(n_{H_2} + n_{He})$ and $p(H_2) = n_{H_2}/(n_{H_2} + n_{He})$ to collide with He atoms or H_2

6

molecules, respectively, with $p(He) + p(H_2)=1$. Then, the fraction of the i-th charge state of heavy ions ($F_i^m=1$) in gas mixtures of He and H_2 will be determined by

$$F_i^m = F_i^{He} \cdot p(He) + F_i^{H_2} \cdot p(H_2). \quad (13)$$

Assuming the equilibration of charge states in gas mixtures, the following expression can be derived from expressions 3 and 9:

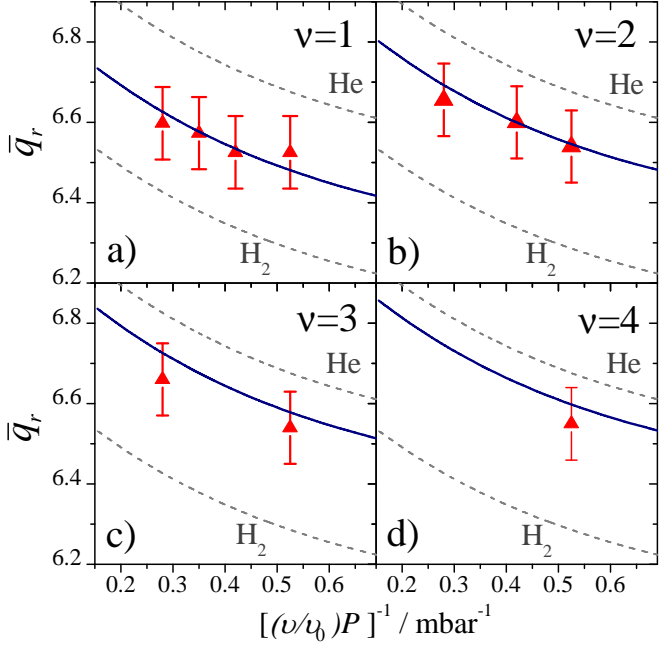$$\bar{q}^m = \bar{q}^{He} \cdot p(He) + \bar{q}^{H_2} \cdot p(H_2) \quad (14)$$

Figure 6: The average charge states of ^{254}No ions depending on pressures of the gas mixtures ν=1, 2, 3 and 4. Experimental values are shown by triangles. Solid curves represent the estimated average charge states from expression (7. Dashed curves represent the average charge states dependence of ^{254}No ions on the pressure of pure He and H_2. See text for details.

where $\bar{q}^{He}$ and $\bar{q}^{H_2}$ are the equilibrated average charge states of No ions in pure He and H_2 at a given pressure P, respectively. This expression is just a weighted mean value of the two equilibrated average charge states in pure He and pure H_2. However, this expression cannot be used directly to obtain the average charge states, as no correction terms for the "density effect" are included. To this end, let us make the assumption that the ratio $\Delta q/\bar{q}$ is constant for He and H_2 at pressures P within (0.2-2.0) mbar based on results from previous subsection (marked by dashed curves in Fig. 6 and Fig. 7). Then the following expression will be valid:

$$\bar{q}_r^m = \bar{q}_r^{He} \cdot p(He) + \bar{q}_r^{H_2} \cdot p(H_2) \quad (15)$$

The average charge states estimated using expression 15 for gas mixtures are shown with solid lines in Fig. 6. The average charge states at various pressures of pure He and H_2 gases were estimated using the parameterized expressions from the previous subsection. The estimated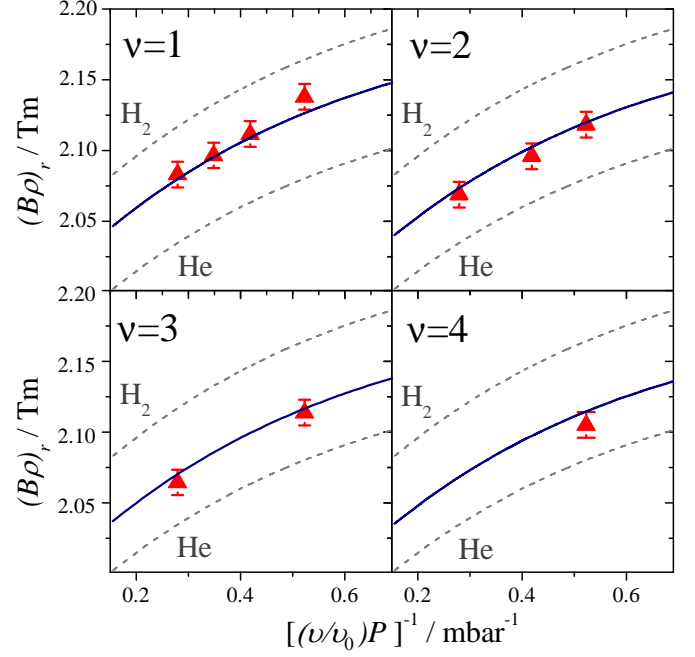 values describe well the average charge states of ^{254}No ions in the gas mixtures over a wide range of gas pressures.

Figure 7: Same as Fig. 6 but for magnetic rigidities. See text for details.

The corresponding magnetic rigidities can also be estimated using expressions 7 and 15. The results are shown in Fig. 7. The magnetic rigidities are also well predicted within a gas pressure range of (1-2) mbar. In the case of gas mixtures, the width of the charge state distribution can be different from that in pure gases due to the different types of ion-atom collisions. However, the observed width is between the values of the pure gases.

5. Summary and Conclusion

The average charge states and magnetic rigidities of ^{188}Pb, ^{252}No and ^{254}No ions produced in the fusion-evaporation reactions ^{48}Ca+^{144}Sm and ^{48}Ca+^{206,208}Pb were investigated at the gas-filled recoil separator TASCA. The gases He, H_2, and their mixture in different ratios were used as filling gas. Measurements were performed at different pressures ranging from 0.2 to 2.0 mbar. In all gases, we observed a strong dependence of the average charge states and magnetic rigidities on the gas pressure. This dependence was attributed to the so-called "density effect". Experimental data were discussed in a simple analytical way and corresponding simple an analytical expression were used for the parameterizations of the data. The results of parameterized expression well describes the behaviour of the average charge states and magnetic rigidities of ^{188}Pb, ^{252}No and ^{254}No ions in pure He and H_2 gases. This effect should be taken into account to predict more precisely the average charge states of heavy ions traveling through dilute gases in gas-filled recoil separators. The ion-optical calculations of the TASCA separator with the "density effect" included describe the experimental

data very well. This is essential to obtain reliable estimates of the transmission of the recoil separator for ERs. The average charge states of heavy ions in gas mixtures were systematically measured for the first time. Using the results from the case of pure He and H_2 gas and also presenting a simple analytical discussion, an expression for the determination of average charge states in a gas mixture was proposed. Results reported in this paper can be used for a better planning of future experiments at gas-filled recoil separators and also for other experimental setups which using the dilute gases at pressures around 1 mbar.

References

[1] H.-D. Betz, Rev. Mod. Phys. **44** (1972) 465.
[2] G. Münzenberg, in Experimental Techniques in Nu-clear Physics, edited by D. N. Poenaru and W. Greiner Walter de Gruyter, Berlin, 1997, p. 375.
[3] Y. T. Oganessian, J. Phys. G 34, (2007) R165 .
[4] K. Morita, et al., J. Phys. Soc. Japan 73, (2004) 2593.
[5] L. Stavsetra, et al., Phys. Rev. Lett. 103, (2009) 132502.
[6] P.A. Ellison, et al., Phys. Rev. Lett. 105, (2010) 182701.
[7] C. E. Düllmann, et al., Phys. Rev. Lett. 104, (2010) 252701.
[8] M. Leino and F.P. Hessberger, Ann. Rev. Nucl. Part. Sci. 54 (2004) 175.
[9] A. Ghiorso et al., Nucl. Instr. and Meth. A 269 (1988) 192.
[10] V. Ninov et al., Nucl. Instr. and Meth. A 357 (1995) 486.
[11] M. Leino, Nucl. Instr. and Meth. B 126 (1997) 320.
[12] Yu. Oganessian et al., Phys. Rev. C 64 (2001) 064309.
[13] K.E. Gregorich et al., Phys. Rev. C 72 (2005) 014605.
[14] H. Miyatake et al., Nucl. Instr. and Meth. B 26 (1987) 309.
[15] J. Khuyagbaatar et al., GSI Sci. Rep. 2009 (2010) 171.
[16] M. Schädel, Eur. Phys. J. D 45 (2007) 67.
[17] M. Schädel, J. Nucl. Radiochem. Sci. 8 (2007) 47.
[18] A. Semchenkov et al., Nucl. Instr. and Meth. B 266 (2008) 4153.
[19] J.M. Gates et al., Phys. Rev. C 83 (2011) 054618.
[20] N. Bohr, Phys. Rev. 58 (1940) 654.
[21] W.E. Lamb, Phys. Rev. 58 (1940) 696.
[22] N. Bohr and J. Lindhard, Kgl. Danske. Videnskab. Selskab, Mat. -fys. Medd., 28, No.7 (1954).
[23] B. Kindler et al., Nucl. Instr. and Meth. A. 561 (2006) 107.
[24] K. Eberhardt et al., Nucl. Instr. and Meth. A. 590 (2008) 134.
[25] B. Lommel et al., Nucl. Instr. and Meth. A. 590 (2008) 141.
[26] J.F. Ziegler, NIM. B 219, (2004) 1027.
[27] Yu. Oganessian et al., Phys. Rev. C 64 (2001) 054606.
[28] S. Hofmann and G. Münzenberg, Rev. Mod. Phys. **72** 733 (2000).
[29] R.B. Firestone, V.S. Shirley, C.M. Baglin, S.Y. Frank Chu, J. Zipkin, Table of Isotopes, 8th Edition, John Wiley & Sons, Inc., New York, Chichester, Brisbane, Toronto, Singapore (1996).
[30] K.E. Gregorich et al., GSI Sci. Rep. 2006 (2007) 144.
[31] L.C. Northcliffe and R.F. Schilling, Nucl. Data Tables A7, (1970) 233